

## Design Considerations for Blast Loads in Pressure Vessels

Edward A. Rodriguez, P.E., Los Alamos National Laboratory  
Robert E. Nickell, Ph.D., Applied Science and Technology  
Jason E. Pepin, Los Alamos National Laboratory

### ABSTRACT

Los Alamos National Laboratory (LANL), under the auspices of the U.S. Department of Energy (DOE) and the National Nuclear Security Administration (NNSA), conducts confined detonation experiments utilizing large, spherical, steel pressure vessels to contain the reaction products and hazardous materials from high-explosive (HE) events. Structural design and analysis considerations include:

- (a) Blast loading phase (i.e., impulsive loading)
- (b) Dynamic structural response
- (c) Fragment (i.e., shrapnel) generation and penetration
- (d) Ductile and non-ductile fracture
- (e) Design Criteria to ASME Code Sec. VIII, Div. 3, Impulsively Loaded Vessels [1]

These vessels are designed for one-time-use only, efficiently utilizing the significant plastic energy absorption capability of ductile vessel materials [2,3]. Alternatively, vessels may be designed for multiple-detonation events, in which case the material response is restricted to elastic or near-elastic range [2-5]. Code of Federal Regulations, Title 10 Part 50 [6] provides requirements for commercial nuclear reactor licensing; specifically dealing with accidental combustible gases in containment structures that might cause extreme loadings. The design philosophy contained herein may be applied to extreme loading events postulated to occur in nuclear reactor and non-nuclear systems or containments.

### INTRODUCTION

Design guidance for extreme loading conditions has been an active pursuit of Section III, Division 1 of the ASME Boiler and Pressure Vessel Code [7]. However, the guidance has been restricted to unlikely extreme loads, known as Level D Service Conditions. An example would be the potential detonation of combustible gases in a containment structure. For the LANL detonation experiments, the concern is expected (likely) extreme loads, which implies substantially different safety margins. As a result, LANL has been actively pursuing a Code Case [8], to develop design guidance for pressure vessels subject to expected blast loads. The containment vessels are used to investigate the high-pressure shock-compression behavior of materials, which is accomplished through application of HE charges to drive metals into an extremely high-strain rate, high-pressure, and high-temperature regime, while the dynamic event is monitored through radiographic ports. In many cases, the explosion products are hazardous, or the materials under compressions are radioactive. This paper describes the necessary design considerations for blast loads in pressure vessels, using analysis results for a 30-lb spherical HE charge inside a 6-ft inner diameter HSLA-100 steel vessel.

### BLAST LOADING PHASE

Impulsive loading developed from a detonation event may be solved through empirical and numerical methods. This section will briefly discuss numerical modeling of hydrodynamic phenomena for containment system design. Empirical methods are widely used in the Department of Defense (DoD) community and are discussed elsewhere [9]. Herein, the hydrodynamic modeling is accomplished using the Sandia National Laboratories (SNL) shock-wave physics code, CTH [10]. CTH is a family of codes for modeling complex multi-dimensional, multi-material problems that are characterized by large deformations and/or strong shocks. Hydrodynamic codes, as the name implies, are based on the fundamental equations of fluid mechanics; conservation of mass, momentum, and energy. For this discussion, only single source HE explosions from bare, spherical, center initiated HE charges will be considered.

**Containment Vessel Model**

Figure 1 shows an ideal HE air blast wave structure. As the blast wave expands, it decays in strength, lengthens in duration, and slows down, both because of spherical divergence and because the chemical reaction is over, except for afterburning, as the high-temperature explosion products mix with the surrounding air [11]. Figure 2 shows a vessel schematic with a spherical charge of PBX-9501 at the center of the vessel.

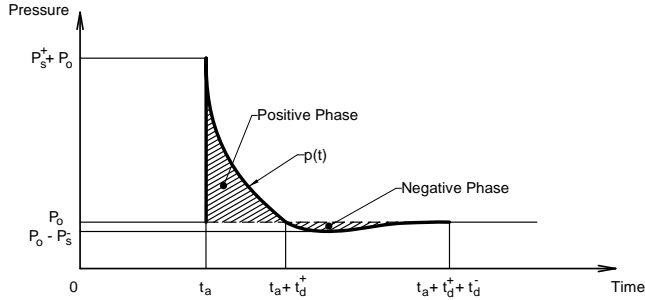


Figure 1. Ideal blast-wave structure

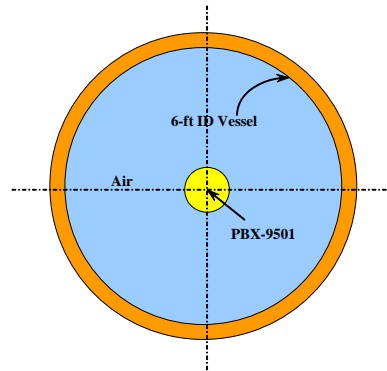


Figure 2. Vessel schematic

The focus is on modeling the 6-ft inner diameter HSLA-100 steel containment vessel to determine the impulsive load developed from detonation of a centrally detonated, bare spherical charge of PBX-9501. An Eulerian mesh encompassing approximately 400,000 cells, shown in Figure 3, represents the mathematical model tracking the pressure, temperature, density, and total energy of the system. Normal air makes up the bulk of the internal vessel volume, and the HSLA-100 vessel shell is modeled as 2.5-inch thick. Figure 3 also depicts details of the entry and exit radiographic beam ports. Tracer particles (i.e., stationary probes) monitor the pressure history of the incident and reflective blast wave, and are embedded in the Eulerian mesh immediately inside the vessel shell, approximately 1.5 cell-widths from the wall. The Jones-Wilkins-Lee (JWL) equation-of-state (EOS) [12] is used for PBX-9501 assuming adiabatic expansion (i.e., steady state expansion at constant entropy).

Strength for the HSLA-100 steel shell is modeled using elastic, perfectly-plastic material model, with minimum yield strength of 100 ksi. A minimum hydrostatic tension failure pressure, or fracture pressure, is also included that provides the required pressure at which void nucleation is induced. Figures 3 through 6 show the progression of the blast wave, from a 30-lb charge of PBX-9501, in terms of reaction products (i.e., gas) density contours. A density decrease is seen from Figure 3 to Figure 4, at the interface of the unshocked air with the unreacted HE and reaction products.

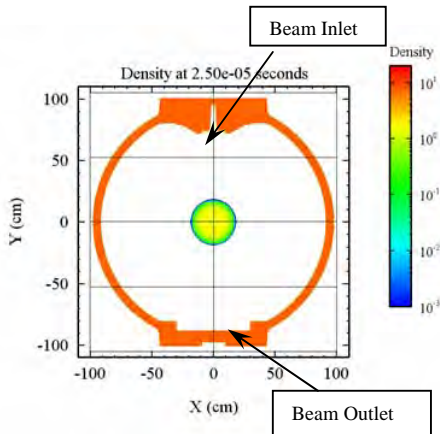


Figure 3. HE burn and detonation at 25 μs.

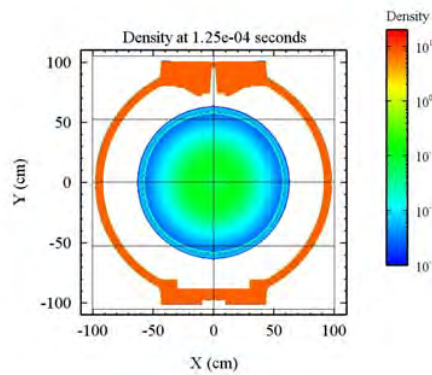


Figure 4. Detonation at 125 μs.

Figure 3 shows the HE burn 25 $\mu$ s after detonation, with much of the charge density still at 1.84 g/cm<sup>3</sup>, but towards the outer contour of the charge, it resembles gas densities. Figure 4 shows the blast wave at 125 $\mu$ s into the transient, with visible density difference radially outward towards the shell wall.

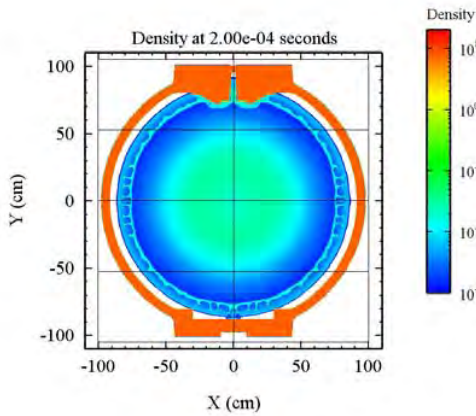


Figure 5. Detonation at 200  $\mu$ s.

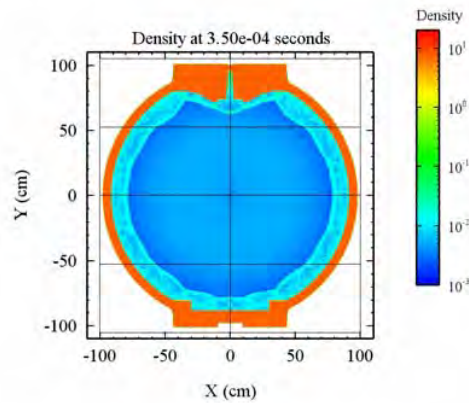


Figure 6. Detonation at 350  $\mu$ s

At about 200  $\mu$ s, the incident blast wave reaches the vessel shell wall, as shown in Figure 5. At this point, the blast wave reflects back towards the center, as shown in Figure 6, thus continuing this process until a steady-state pressure has remained. Figures 7 and 8 show the average P-T history from all tracer points within the free-field of the vessel shell for 30lb and 40lb bare spherical charge of PBX-9501. No tracer points in the vicinity of the radiographic beam inlet or outlet were used in averaging. For visual clarity, the time scale on the P-T history plots have been scaled upward by 1ms. As such, when the detonation blast wave first strikes the vessel wall at 200 $\mu$ s (see Figure 5), the actual time shown in Figure 7 and Figure 8 corresponds to 1200 $\mu$ s (or 1.2ms).

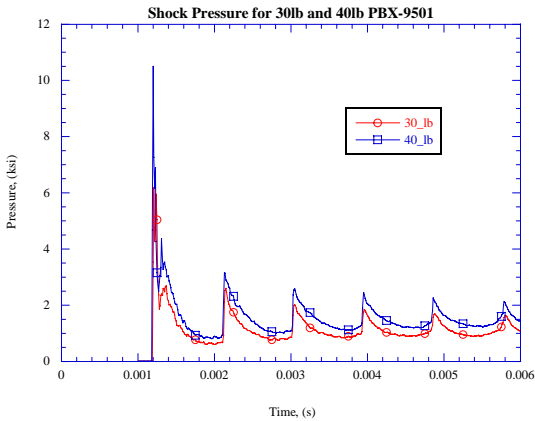


Figure 7. P-T history of 30 and 40-lb. spherical charge.

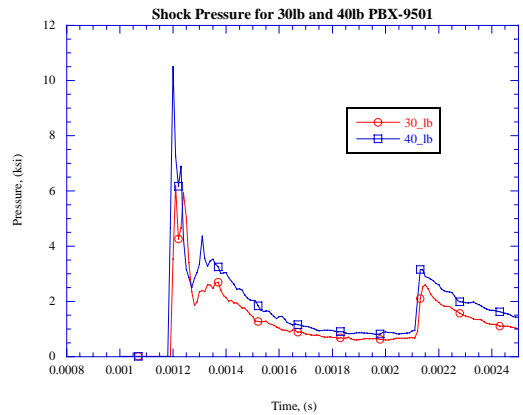


Figure 8. P-T history of 30lb & 40lb – expanded time scale.

Gas expansion and contraction within the vessel produces the subsequent peak pressure reverberations, as seen in Figure 7. The area under the P-T curve represents the total specific impulse in the system, excluding the pseudo-static pressure. The resulting P-T data is the input function to the structural model. It should be noted that

## DYNAMIC STRUCTURAL RESPONSE

The dynamic analysis is accomplished using the explicit finite-element code ParaDyn, which is the massively parallel version of DYNA3D [13]. Resulting P-T history from CTH hydrodynamics code is input to the structural dynamics code. DYNA3D is a non-linear, explicit, Lagrangian finite element analysis code used for three-dimensional transient structural mechanics. Numerical simulation requires the use of large, detailed meshes in order to include engineering features such as the bolted port connections. The vessel, shown in Figures 9 and 10, is a 72-inch inside diameter, 2.5 inch thick spherical shell with 5 ports. Each port has a steel cover bolted to a nozzle with 72-1.25-inch diameter bolts. The four side ports are entry/exit locations for the x-ray beams, and contain radiographic hardware and fragment shielding. The fifth port on top of the vessel is used for general access. Welded areas of the vessel, including the nozzle-to-vessel welds and the girth weld, are included in the model and appear as magenta regions.

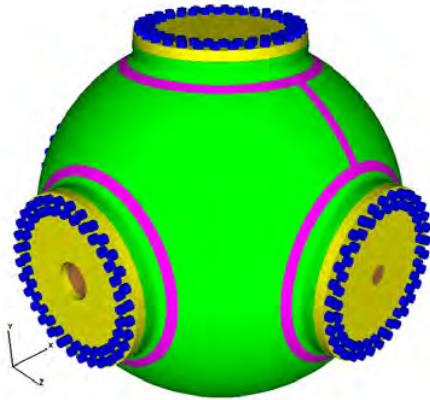


Figure 9: Vessel analysis model.

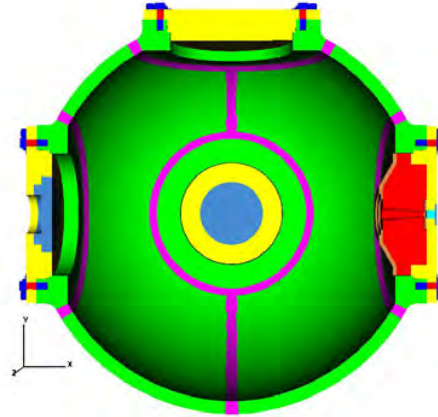


Figure 10: Cut-away view of model.

The finite element model consists of ~5.7 million hexahedral elements. Tied contact has been used in place of screw-threads to hold the bolts to the nozzle. Thermal strain is applied to the blue shaded elements (between the “threaded” region in the nozzle and the bolt head) during the first millisecond of the analysis to place bolts in tension, thereby approximating a bolt torque of 1,100 ft-lbs. A tabular elastic-plastic material model is used to model the HSLA-100 steel, beryllium, and AL 7050-T7451. A bi-linear elastic-plastic material model was used to model the bolt steel and an elastic material model was used for the tungsten. Stress-strain plots for all of the models for these materials are shown in Figure 11.

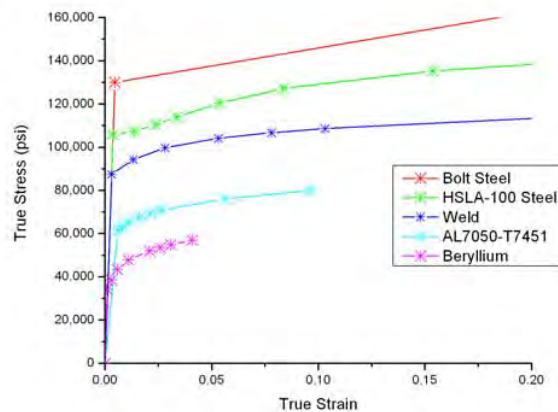


Figure 11: Stress-strain curves used to model the vessel materials.

### Structural Response Results

The large initial pulse from the HE causes the confinement vessel to initially expand and contract in a “breathing mode,” an almost uniform radial expansion of the entire vessel and ports. Due to the large masses of the nozzles and doors, the breathing mode quickly degenerates into a more complex combination of bending/extensional modes. Duffey [2] has shown that even for a pristine spherical shell without any perturbation, such as added masses or nozzles, there are numerous bending

modes above and below the so-called fundamental (i.e., breathing) mode. Figure 12 shows localized bending at 3.5 ms, which cause large stresses on the spherical shell between the ports. Localized bending stresses are significantly greater than the stresses caused by the initial breathing pulse. Figure 13 shows the bolt deformation on the top cover, with significant bolt-bending.

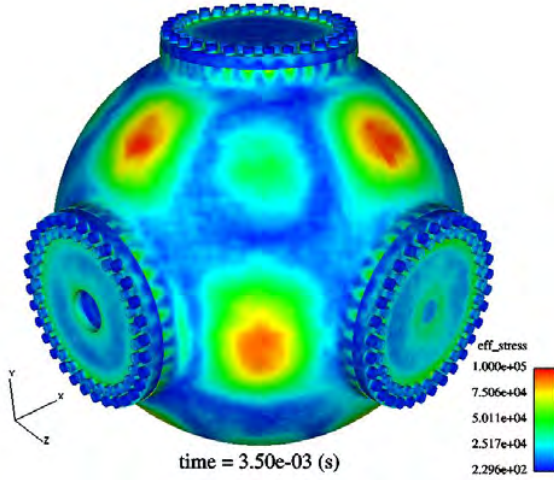


Figure 12: Equivalent stresses (bending modes).

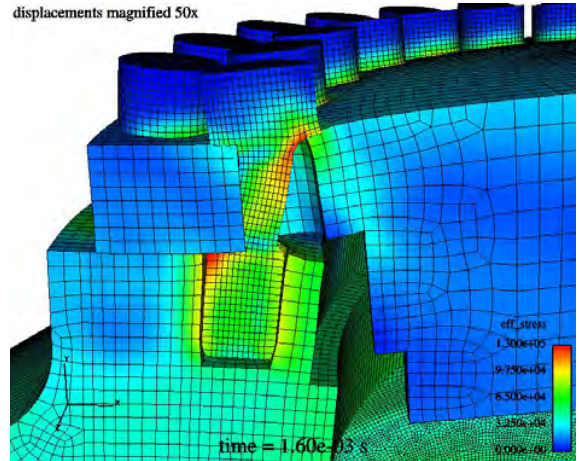


Figure 13: Bolts deformation at top port. (Deformations are exaggerated by a factor of 50)

As the initial blast wave impinges and expands the vessel in a breathing mode response, pure membrane strains are developed throughout the shell. These early-time strains are a fraction of late-time strain exhibited in localized bending. Although peak bending strains cause localized plasticity at numerous locations, there is no single late-time mechanism to cause gross shell failure.

**FRAGMENT LOADING**

When high-explosive (HE) intimately contacts its surrounding steel casing, extremely high-velocity fragments are ejected during the dynamic fracture process. Figure 14 shows the time-sequence events, where the blast wave reached the vessel shell 250μs after detonation. Fragments arrive at the vessel shell at about 420μs. Figure 15 depicts the fragment cloud, conservatively assuming all fragments impact the vessel wall simultaneously for maximum response.

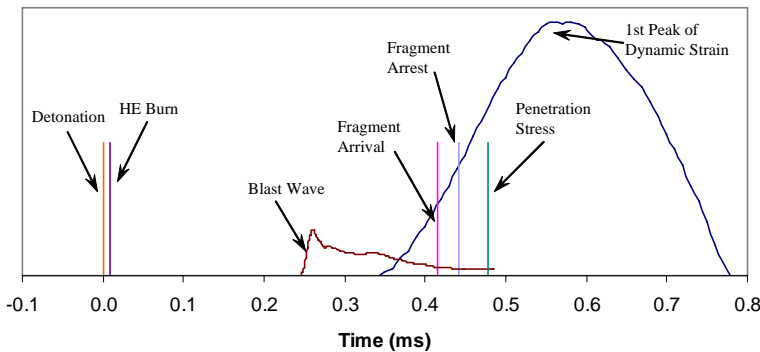


Figure 14. Time sequence of events during detonation and fragment impact.

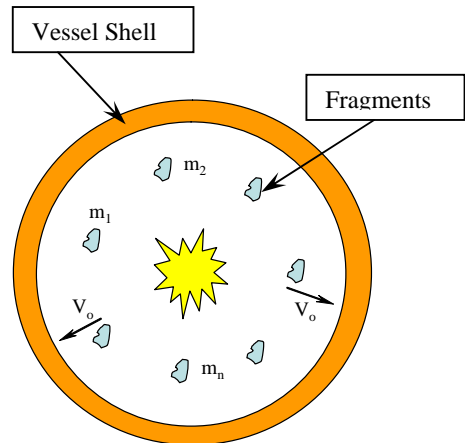


Figure 15. Fragment cloud schematic.

Fragments could partially penetrate or completely perforate the steel vessel shell. As such, design consideration should focus on the required steel shell thickness to prevent perforation, or likewise, take advantage of fragment shielding in the inner shell wall. There are two time-lagged superimposed events that must be considered in the design; (a) the blast wave (see Fig. 7), and (b) fragment field (or fragment cloud) impacting the vessel shell. Structural vessel response must include the effects of the fragment cloud. For typical vessel conditions analyzed herein, the fragment cloud impulse is approximately 15-25% of the blast wave impulse.

To determine potential damage from a single fragment, Figure 16 shows a numerical simulation utilizing CTH, of a depleted uranium (DU) fragment impacting the HSLA-100 steel vessel shell. The 6-cm long fragment impacts at 2.0km/s and penetrates almost completely through the thickness of the shell.

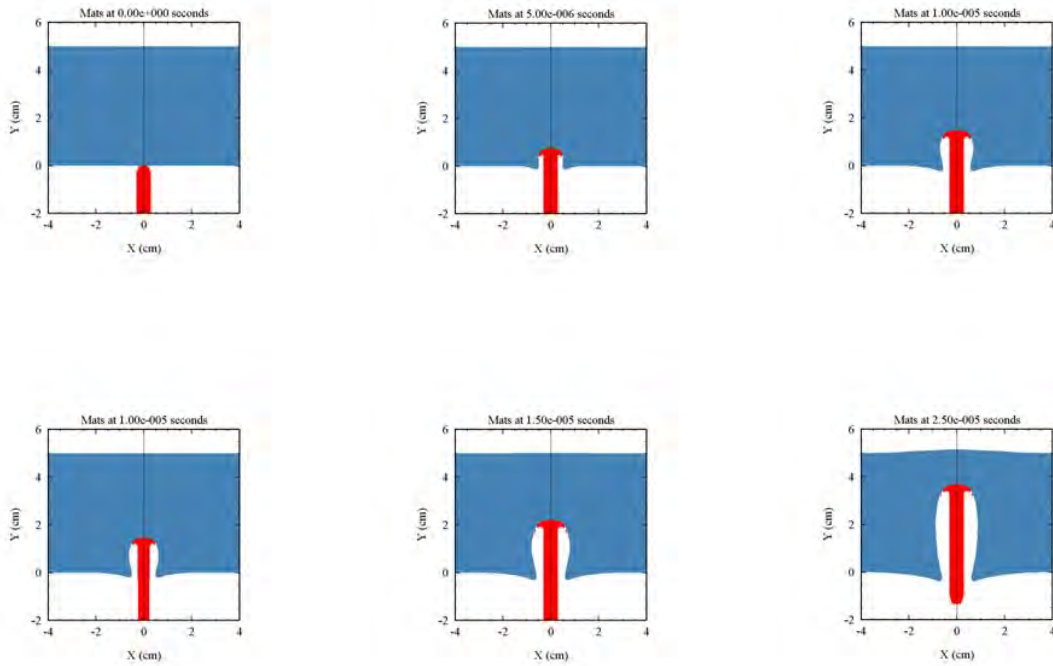


Figure 16. Depleted uranium fragment penetrating HSLA-100 steel.

Typical fragment velocities can be readily calculated based on the Gurney method for simplified casing geometries [14] and typical fragment sizes are determined via two methods; (a) a Mott distribution [15] for fragment mass, and (b) Grady-Kipp dynamic fracture theory [16]. The Mott distribution provides the total number of fragment for a given relative fragment mass, while the Grady-Kipp dynamic fracture theory provides an average geometric spacing (i.e., size).

## DUCTILE AND NON-DUCTILE FRACTURE

Extreme loads, such as blast and fragment impact, may be severe enough to cause ductile or non-ductile fracture of the shell or nozzle component. Fatigue crack growth calculations, in accordance with ASME Section VIII, Division 3, KD-4 are required because no credit can be taken for leak-before-burst under rapid impulsive loads. That is, a vessel response under an impulsive event is much too rapid for a leak to be an adequate indicator of a potential burst and any leak could turn to burst before any action could be taken. As a result, within the logical framework, the crack growth rules of KD-4 are invoked for fatigue crack-growth assessment rather than the crack initiation rules of Section VIII, Division 3, KD-3.

Detailed numerical computations, or simplified elastic-plastic analyses utilizing the API-579 methodology [17], must be employed to determine design adequacy. Figure 17 depicts a finite element analysis of the 6-ft ID HSLA-100 vessel subjected to the impulsive event of Figure 7, with an embedded part through-wall flaw at the vessel north-pole. The flaw is shown to attain crack-tip plasticity

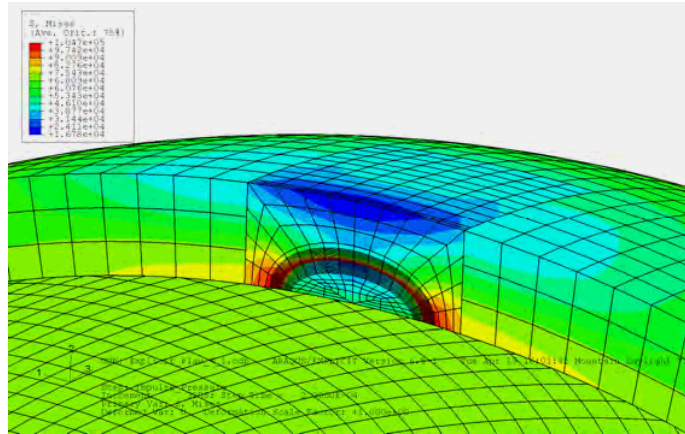


Figure 17. – Part through-wall flaw in vessel subject to impulse loads.

To deal with the high primary load, a simplified elastic-plastic fracture assessment, such as that of API 579 [17] using a fracture assessment diagram (FAD) is recommended. This simplification assumes a flaw can exist anywhere in the vessel in the worst orientation by determining only the absolute largest values of stress throughout the vibration time-history following an impulse event, irrespective of direction. The simplification defines a single, through-wall, stress that bounds the actual stresses at all times during the transient at the section for fracture assessment.

### ASME CODE DESIGN CRITERIA

The analysis results described in the preceding paragraphs can be compared with the existing design requirements of the ASME Code Section VIII, Division 3 [1]. However, the more appropriate design requirements are contained in a Code Case [8], currently under consideration by the ASME Code Section VIII, that would provide design rules specifically for vessels subject to impulsive loads, such as those caused by internal detonations. This Code Case is in the final stages of deliberation, with final balloting expected in May 2007. The Code Case includes a requirement to demonstrate margin against global plastic instability, with a factor of safety of 1.732. As an example, this margin may be demonstrated by an elastic-plastic dynamic analysis, with an impulse equal to 175 % of the design-basis impulse, which does not result in the formation of a mechanism (e.g., the formation of a complete plastic hinge around an opening or closure). Furthermore, the Code Case also requires cumulative membrane, bending, and peak strain limits (for multiple strain cycles within a single detonation, as well as strains accumulated from multiple detonations) that protect the vessel wall neutral axis and also prevent local ductile tearing.

For example, vessels subjected to, either single or multiple, impulsive loading events, the in-plane plastic strain components shall be accumulated over strain cycles within a single loading event, or strain cycles within successive loading events, respectively. The maximum in-plane equivalent plastic strain during the transient, averaged through the thickness of the vessel, as the result of the design basis impulsive loading shall not exceed 0.2 %. The maximum in-plane equivalent plastic strain during the transient, linearized through the thickness of the vessel, as the result of the design basis impulsive loading, shall not exceed 2 % (1 % at welds). The maximum peak equivalent plastic strain during the transient at any point in the vessel, as the result of the design basis impulsive loading, shall not exceed 5 % (2.5 % at welds). Also, the designer shall consider the need to reduce these strain limits for areas of high biaxial or triaxial tension. In addition to limits that prevent ductile failure, the Code Case also contains requirements that prevent non-ductile failure modes, such as unstable crack propagation. The Code Case does not provide specific limits for potential fragment penetration, other than a requirement that, for multiple detonation loading events, the fragment penetration from a prior detonation cannot be greater than the

assumed initial flaw used for the unstable crack propagation assessment. If this requirement cannot be met, a protective liner is required for any subsequent detonations.

## SUMMARY

This paper has described the necessary design considerations for blast loads in pressure vessels, by utilizing a design example of a 30-lb PBX-9501 HE charge with a metal casing, detonating inside a 6-ft inner diameter HSLA-100 steel vessel. First, blast impulse loads are determined using computational hydrodynamic methods. These impulse loading functions are then used in an explicit dynamics finite element model to determine the structural response. Blast and fragment loading must be considered together for an overall impulse to the system. Fragment generation and potential penetration must also be assessed to determine likelihood of perforation. Finally, ductile and non-ductile failure assessment is accomplished with simplified methods or computational models. It is important to note that ASME Boiler and Pressure Vessel, Section VIII, Code Case will provide guidance for these extreme load events. Utilizing the Code Case rules and regulations as currently written, the vessel design noted herein meets all the requirements.

## REFERENCES

- [1] ASME Boiler and Pressure Vessel Code, Section VIII, Division 3, Pressure Vessels – Alternative Rules, American Society of Mechanical Engineers, New York, NY, 2006.
- [2] Duffey, T. A., Rodriguez, E. A., and Romero, C., “Design of Pressure Vessels for High Strain-rate Loading: Dynamic Pressure and Failure Criteria,” *Welding Research Council*, Bulletin No. 477, December 2002.
- [3] Rodriguez, E. A. and Duffey, T. A. Fracture-Safe and Fatigue Design Criteria for Detonation-Induced Pressure Loading in Containment Vessels,” *Welding Research Council*, Bulletin No. 494, August 2004.
- [4] Baker, W. E. “The Elastic-Plastic Response of Thin Spherical Shells to Internal Blast Loading,” *Journal of Applied Mechanics*, Vol. 27, pp. 139-144 (1960).
- [5] White, J. J. and Trott, B.D., “Scaling law for the Elastic Response of Spherical Explosion-Containment Vessels,” *Experimental Mechanics*, Vol. 20, 174-177 (1980).
- [6] Code of Federal Regulation, Title 10, Energy, Chapter I, Nuclear Regulatory Commission, Part 50 – Domestic Licensing of Production and Utilization Facilities, 2006.
- [7] ASME Boiler and Pressure Vessel Code, Section III, Division 1, Appendix F, Nuclear Pressure Vessels, American Society of Mechanical Engineers, New York, NY, 2006.
- [8] ASME Boiler and Pressure Vessel Code, Section VIII, Division 3, Special Working Group on High-Pressure Vessels, Task Group on Impulsively Loaded Vessels, R. E. Nickell, Chairman, 2007.
- [9] Rodriguez, E. A. and Romero, C., “Hydrodynamic Modeling of Detonations for Structural Design of Containment Vessels,” *Proceedings of PVP2006-ICPVT-11, ASME Pressure Vessels and Piping Division Conference*, July 23-27, 2006, Vancouver, British Columbia, Canada.
- [10] Hertel, E. S., Bell, R. L., Elrick, M. G., Farnsworth, A. V., Kerley, G. I., McGlaun, J. M., Petney, S. V., Silling, S. A., Taylor, P. A., and Yarrington, L., “CTH: A Software Family for Multi-Dimensional Shock Physics Analysis,” in *Proceedings of the 19th International Symposium on Shock Waves*, held at Marseille, France, July 1993, pp. 377-382
- [11] United States Department of Energy, *A Manual for the Prediction of Blast and Fragment Loadings on Structures*, DOE/TIC-11268, US Department of Energy, Albuquerque Operations Office, Amarillo Area Office, Pantex Plant, July 1992.
- [12] Cooper, P. W., *Explosives Engineering*, VCH Publishers, New York, NY, 1996.
- [13] Whirley, R. and Engelmann, B., “DYNA3D User Manual,” Lawrence Livermore National Laboratory report UCRL-MA-107254, Rev. 1 (Dec. 1998).
- [14] Loyd, R. M., Ed., Conventional Warhead Systems Physics and Engineering Design, *Progress in Astronautics and Aeronautics, Volume 179*, American Institute of Aeronautics and Astronautics (AIAA), 1998
- [15] Mott, N. F., “Fragmentation of Shell Cases,” *Proceedings of the Royal Society of London, Series A, Mathematical and Physical Sciences*, Vol. 189, June 1947.
- [16] Davison, L., Grady, D. E., and Shahinpoor, M., *High-Pressure Shock Compression of Solids II - Dynamic Fracture and Fragmentation*, Springer, New York, NY, 1995.
- [17] API-579, *Fitness for Service*, American Petroleum Institute, 2000.